NASA Technical Memorandum 83147

APPROXIMATE ANALYSIS OF POSTBUCKLED THROUGH-WIDTH DELAMINATIONS

John D. Whitcomb

June 1981

National Aeronautics and Space Administration

Langley Research Center
Hampton, Virginia 23665

APPROXIMATE ANALYSIS OF POSTBUCKLED THROUGH-WIDTH DELAMINATIONS

John D. Whitcomb
NASA Langley Research Center
Hampton, Virginia 23665

SUMMARY

An approximate analysis was developed to analyze the postbuckling behavior of through-width delaminations in a laminated coupon. The analysis contains two parameters which are determined using a finite element analysis. After calculating the parameters for a few configurations, the approximate analysis was used to analyze many other configurations. Lateral deflections and mode I strain-energy release rates obtained with the approximate analysis were compared with results from the finite element analysis. For the configurations analyzed, the approximate analysis agreed very well with the finite element results.

INTRODUCTION

In laminated composite structures under compression loads, delaminations often precipitate failure. Even small, seemingly benign delaminations may induce localized buckling, which causes high interlaminar stresses. A buckled delaminated region may grow rapidly and lead to structural instability. To assess the criticality of a delamination, an analysis is needed to predict the rate of instability-related delamination growth. A key component of any such analysis is an accurate geometrically-nonlinear stress analysis. Unfortunately, general purpose analyses, such as geometrically-nonlinear finite element analysis, tend to be expensive. Specialized inexpensive approximate analyses are needed.

This paper presents an approximate analysis for postbuckling of through-width delaminations in a laminated composite coupon (fig. 1). This configuration

is perhaps the simplest that exhibits instability-related delamination growth. Hence, it is an ideal candidate for initial study. Furthermore, this configuration was studied in reference 1 using a geometrically-nonlinear finite element analysis. Thus, reference solutions are available. In the following sections the development of an approximate analysis is outlined. Lateral deflections and mode I strain-energy release rates obtained with the approximate analysis are compared with results obtained with the analysis described in reference 1.

NOMENCLATURE

A_A	cross-sectional area of region A, m^2
2a	length of delamination before loading, m
2a'	effective length of delamination before loading, m
$2\bar{a}$	axial length of delamination after loading, m
b	width of coupon, m
C_1, C_2	constants used in calculating G_I
E	Young's modulus, GPa
E_A, E_D	extensional moduli for regions A and D, GPa
G_I	mode I strain-energy release rate, J/m^2
G_D	transverse shear modulus of region D, GPa
G_M	strain-energy release rate due to a moment, J/m^2
I	moment of inertia, m^4
I_D	moment of inertia of region D, m^4
M	moment, N•m
M_c	crack closing moment, N•m
M_o	crack opening moment, N•m

n	shape factor equal to 1.2 (ref. 2)
P_A, P_B, P_C, P_D	axial loads in regions A, B, C, and D, N
P_{FE}	buckling load calculated using finite element analysis, N
P_T	applied load, N
$\overline{P}_T$	applied load corresponding to incipient buckling, N
t	thickness of delaminated region, m
x,y	rectangular Cartesian coordinates, m
δ	maximum lateral deflection of buckled region, m
$\hat{\delta}$	lateral deflection corresponding to peak G_I, m
$\tilde{\delta}$	lateral deflection corresponding to closing of crack tip, m
ε_A	axial strain in region A
ε_D	midplane axial strain in region D

ANALYSIS

Development of Governing Equations

In this section approximate governing equations are derived for a laminate with a postbuckled through-width delamination. The laminate was subdivided into four regions, as shown in figure 2. Because of symmetry, only half of the laminate was modeled. The laminate was assumed to be of width b. Regions B and C are assumed to be perfectly bonded. Regions A and D are unbonded. Regions A, B, and C have constant axial strain. Hence, the force-displacement relations are those for a simple rod subjected to axial load. Region D is assumed to have zero slope at both ends. To describe the nonlinear behavior of region D, equations (1) and (2) for postbuckling of a column were used.

$$P_D = \frac{\pi^2 E_D I_D}{a^2} \left(1 + \frac{n\pi^2 E_D I_D}{a^2 A_D G_D}\right)^{-1} \qquad \text{ref. (2)} \tag{1}$$

$$a - \bar{a} = a \left[\frac{P_D}{A_D E_D} + \frac{\pi^2 \delta^2}{16 a^2}\right] \qquad \text{ref. (3)} \tag{2}$$

where δ, a, $\bar{a}$, and P_D are lateral deflection, axial length before and after deformation, and load, respectively. Equations (1) and (2) were derived using a strength of materials analysis of a column.

To combine regions A, B, C, and D, equilibrium and compatibility conditions must be considered. The equilibrium condition for the axial force is

$$P_A + P_D = P_B + P_C = P_T \tag{3}$$

Compatability requires the shortening of regions A and D to be identical. Hence,

$$\frac{P_A a}{E_A A_A} = a - \bar{a} \tag{4}$$

Equations (2), (3), and (4) can now be combined to obtain the governing equation for the laminate in terms of one unknown, δ.

$$\frac{\left(P_T - P_D\right)}{E_A A_A} = \left(\frac{P_D}{A_D E_D} + \frac{\pi^2 \delta^2}{16a^2}\right) \tag{5}$$

Equation (5) can be solved explicitly to obtain δ.

$$\delta = \frac{4a}{\pi}\left(\frac{P_T - P_D}{A_A E_A} - \frac{P_D}{A_D E_D}\right)^{1/2} \tag{6}$$

In a later section, lateral deflections calculated with equation (6) will be compared with results obtained with a finite element analysis.

Calculation of Mode I Strain-Energy Release Rate

In reference 1 the mode I strain-energy release rate (G_I) was shown to dominate instability-related delamination growth. The complexity of the load transfer at the crack tip prevents a simple, exact calculation of G_I. An approximate procedure is presented here.

Transverse normal stress at the crack tip is the net result of two opposing processes. The lateral deflection, δ, causes a moment M_o which tends to open the crack tip. M_o can be calculated by considering moment equilibrium of region D (see sketch below).

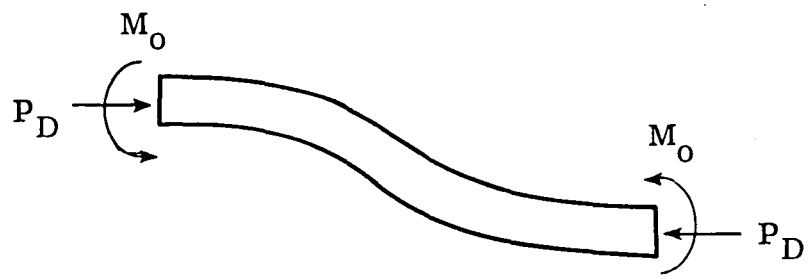

M_o is found to be

$$M_o = \frac{1}{2} P_D \delta \tag{7}$$

After the delaminated region buckles, an increase in applied load causes no change in the load carried by the buckled column (region D in the sketch), (see eq. (1)).

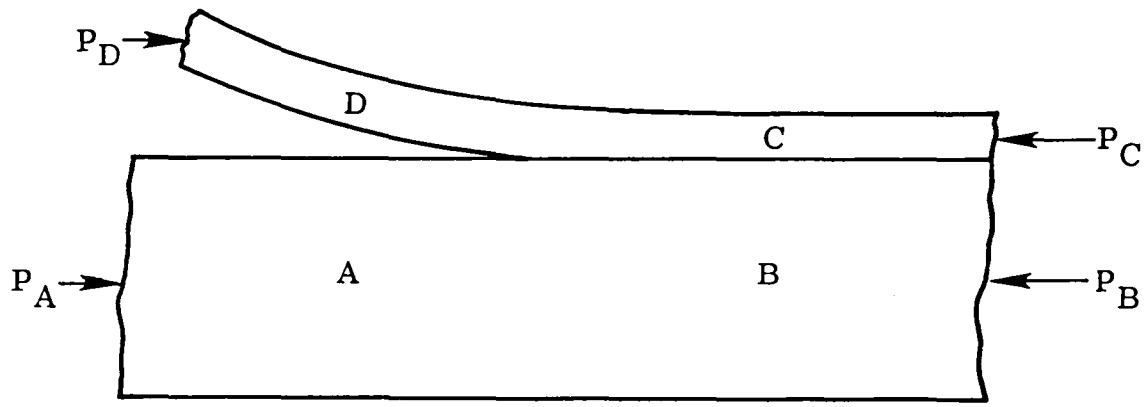

But the load carried by region C continues to increase with increased applied load. Hence, load must be transferred from C to A. The eccentricity in the load path causes a moment, M_c, which tends to close the crack tip. Because the closing moment arises from the difference in axial forces in regions C and D, M_c is expected to be strongly dependent on the quantity $(P_C - P_D)$. Hence, the closing moment is assumed to be

$$M_c = -C_1 \frac{t}{2} (P_C - P_D) \tag{8}$$

The constant C_1 is difficult to determine analytically because it depends on the complex stress diffusion process at the delamination front.

In the present method, it is left as a free constant to be determined through finite element analysis.

The strain-energy release rate for a cantilever beam loaded by a moment is $M^2/2EIb$ (ref. 4). Assuming region D to behave like a cantilever beam, the strain-energy release rate associated with the moments M_o and M_c is

$$G_M = \frac{(M_o + M_c)^2}{2E_D I_D b} \tag{9}$$

However, G_I is not necessarily equal to G_M. Because the specimen is not symmetric about the delamination, the moments can create both normal and shear stresses. Assuming the behavior near the crack tip is linear, G_I is a constant fraction of G_M.

$$G_I = C_2 G_m \tag{10}$$

Combining equations (6) through (10) and using the rule of mixtures to calculate P_C, G_I can be expressed in terms of δ as

$$G_I = \frac{C_2 \left\{ \frac{1}{2} P_D \delta - C_1 \frac{t}{2} \left[\frac{E_D A_D}{E_D A_D + E_A A_A} \left(\frac{P_D}{A_D E_D} (E_D A_D + E_A A_A) + \frac{A_A E_A \pi^2 \delta^2}{16 a^2} \right) - P_D \right] \right\}^2}{2E_D I_D b} \tag{11}$$

The constants C_1 and C_2 in equations (8), (10) and (11) have to be calculated with a finite element analysis; the procedure for calculating them will be discussed in a later section.

Extremum Behavior of G_I

Reference 1 showed that G_I initially increases with increasing load and lateral deflection and then decreases. Since finite elements were used, no closed form expression was obtained to describe this behavior. In this section equations are presented which describe when G_I first becomes nonzero (i.e., initial buckling), the load and deflection for peak G_I, the peak value of G_I, and the load and deflection for closure of the crack tip (which results in zero G_I).

Initial buckling occurs when the load carried by the delaminated region, P_D, reaches the buckling load. Until buckling occurs, the load carried by the delaminated region is linearly related to the remote load.

$$P_D = P_T \frac{A_D E_D}{A_D E_D + A_A E_A} \tag{12}$$

Equating equations (1) and (12) yields an expression for the applied load for incipient buckling (and hence nonzero G_I).

$$\bar{P}_T = \frac{\pi^2 E_D I_D}{a^2} \quad \frac{A_D E_D + A_A E_A}{A_D E_D} \quad \left(1 + \frac{n\pi^2 E_D I_D}{a^2 A_D G_D}\right)^{-1} \tag{13}$$

The maximum value of G_I occurs when the total peeling moment, $(M_o + M_c)$, reaches a maximum. The maximum value for $(M_o + M_c)$ is found by solving equation (14)

$$\frac{\partial}{\partial P_T}(M_o + M_c) \equiv \frac{P_D}{2} \frac{\partial \delta}{\partial P_T} - \frac{C_1 t}{2} \frac{\partial P_C}{\partial P_T} = 0 \tag{14}$$

The term $\frac{\partial \delta}{\partial P_T}$ is calculated from equation (6); the term $\frac{\partial P_C}{\partial P_T}$ is calculated using equation (3) and the rule of mixtures. Solving equation (14), one obtains the lateral deflection corresponding to peak G_I, $\hat{\delta}$.

$$\hat{\delta} = \frac{8a^2 P_D (A_D E_D + A_A E_A)}{\pi^2 A_A E_A A_D E_D C_1 t} \tag{15}$$

The corresponding applied load is obtained by solving equation (6) for P_T, that is

$$P_T = \frac{P_D}{A_D E_D} (A_D E_D + A_A E_A) + \frac{A_A E_A \pi^2 \delta^2}{16a^2} \tag{16}$$

The peak value of G_I is calculated using $\hat{\delta}$ in equation (11).

To determine the load and deflection at which the crack tip closes, equation (17) is solved.

$$M_o + M_c = 0 \tag{17}$$

Substituting expressions for M_o and M_c into equation (17) (using equation (3), rule of mixtures, and equation (16) to express P_C as a function of δ) results in

$$\tilde{\delta} = \frac{16a^2 P_D (A_D E_D + A_A E_A)}{\pi^2 A_A E_A A_D E_D C_1 t} \tag{18}$$

Note that $\tilde{\delta} = 2\hat{\delta}$. The corresponding applied load is calculated by using $\tilde{\delta}$ in equation (16).

Calculation of Constants, C_1 and C_2

Finite element solutions are required to determine the constants C_1 and C_2. The finite element analysis is discussed briefly in a later section.

To calculate C_1, equation (15) was used. Finite element analysis was used to determine the lateral deflection, δ, at which G_I is maximized for a particular configuration.

After calculating C_1, C_2 was calculated using equation (10). G_M was calculated with equation (9) and G_I was calculated with the finite element analysis. G_M and G_I were calculated at the lateral deflection corresponding to the maximum G_I for a particular configuration.

C_1 and C_2 could have been calculated using any two points, but the calculations would have been more tedious.

Both constants were found to be independent of the delamination length and load; C_1 was also independent of the thickness of the buckled region. Consequently, G_I can be calculated with the approximate analysis for many different configurations after studying a few configurations with the finite element analysis.

Modifications for Short, Thick Delaminated Regions

If the buckled region is short and thick, the analysis described in the preceding sections should be modified to account for rotation at the ends of the delaminated region. Clamp conditions were assumed to obtain equation (6).

Rotation at the ends of the delamination cause the delamination to behave like it is longer than it is. That is, the buckling load is lower and the lateral deflection is greater than for the case of clamped ends. The effective lengthening can be estimated from the relative magnitudes of P_D calculated with equation (1) and the buckling load calculated by a finite element analysis. If we ignore the small shear correction term $\left(\frac{n\pi^2 E_D I_D}{a^2 A_D G_D}\right)$ in equation (1), P_D is inversely proportional to a^2. Hence, the effective length is approximately

$$2a' = 2a\left(\frac{P_D}{P_{FE}}\right)^{1/2} \tag{19}$$

Finite Element Analysis

A two-dimensional, geometrically nonlinear finite element analysis was used to obtain rigorous reference solutions. These solutions were used to calculate C_1, C_2, and $2a'$ for use in the approximate solution. The solutions were also used to determine the accuracy of the approximate analysis.

The finite element analysis is described in detail in reference 1. A typical finite element mesh is shown in figure 3. The mesh contained 813 nodes and 740 four-node isoparametric elements. Similar meshes were used for other delamination lengths (2a) and depths (t). Strain-energy release rates were calculated using the crack closure technique reported in reference 5.

Description of Specimen Configuration

The specimen configuration used in the parametric analysis consisted of unidirectional graphite/epoxy (regions C and D in fig. 2) bonded to an aluminum bar (regions A and B in fig. 2). The graphite/epoxy had a thickness t (see fig. 1). The aluminum had a thickness of 6.0 mm. The Young's moduli and shear modulus were assumed to be:

aluminum: $E = 67$ GPa (9.7×10^6 PSI)

graphite/epoxy: $E = 140$ GPa (20×10^6 PSI)

$G = 5.9$ GPA ($.85 \times 10^6$ PSI)

RESULTS AND DISCUSSION

The objective of this section is to illustrate the potential of the approximate analysis for analyzing specimens containing through-width delaminations. Specimens with different delamination lengths, delamination depths (t), and applied loads were analyzed. A finite element analysis was used to obtain reference solutions.

Two calculated parameters were examined--lateral deflections and mode I strain-energy release rate (G_I). The lateral deflection was considered an important parameter for study because intuitively one might expect the severity of the interlaminar stresses to be related to the degree of post-buckling. Also the accuracy of the calculated lateral deflection (determined by comparison with finite element results) is a measure of how well the gross deformation behavior of the specimen is modeled. G_I was considered

because results presented in reference 1 suggested that delamination growth rates are dominated by G_I.

In the results presented, corrections for end rotation are not included except where specifically indicated. This was done so that the simplest form of the approximate analysis could be evaluated.

Figures 4 through 6 show calculated lateral deflections δ for various delamination lengths, delamination depths, and applied loads. The approximate analysis (eq. (6)) and the finite element analysis agree very well for most of the cases. The differences are primarily a result of rotation at the ends of the delamination. The rotation is greatest for the case $t = 0.762$ mm. Since ignoring end rotation "stiffens" the system, it is not surprising that the finite element analysis always predicted a lower buckling load and a greater deflection.

Figure 7 shows that for $t = 0.762$ mm the approximate and finite element analyses agree very well if corrections are included for end rotation. For both $2a = 25.4$ mm and $2a = 38.1$ mm the difference between the effective length and actual length of the delamination was calculated (with eq. (19)) to be approximately

$$(2a' - 2a) \cong 2t \tag{20}$$

Figures 8 to 11 compare mode I strain-energy release rates calculated with the approximate analysis (eq. (11)) and the finite element analysis. Figure 8 shows the relationship between G_I, lateral deflection, and delamination length for $t = 0.508$ mm. The constants C_1 and C_2 were calculated (as described earlier) using only the finite element results for

the case $2a = 25.4$ mm. The figure shows the approximate analysis agrees very well with the finite element results for all four delamination lengths.

Figures 9 through 11 show the relationship between G_I, applied load, and delamination length. Three values of t are examined: 0.508, 0.254, and 0.762 mm. The value of the constant C_1 determined from figure 8 (in which $t = 0.508$ mm) was used for all three values of t. C_2 had to be calculated for each value of t. The finite element results for the shortest delamination length (for each t) were used to calculate C_2.

The analyses agree very well for the cases $t = 0.508$ mm (fig. 9) and 0.254 mm (fig. 10). For $t = 0.762$ mm (fig. 11) the agreement is fair. Recall that when lateral deflections were calculated, the approximate analysis was not as accurate for the case $t = 0.762$ mm. However, with the corrections for end rotations, the approximate analysis performed very well even for $t = 0.762$ mm. If these corrections are used, the G_I calculations also are greatly improved, as shown in figure 12. To determine how these corrections might affect calculations for other values of "t," the curves in figure 9 were recalculated using the corrections for end rotations. Equation (20) was used to determine the effective length (instead of eq. (19)). Comparison of figures 9 and 13 shows the approximate analysis agrees more closely with the finite element analysis if end rotation effects are included.

CONCLUDING REMARKS

An approximate analysis for postbuckling of a through-width delamination in a laminated composite coupon was developed. Lateral deflections and mode I strain-energy release rates (G_I) obtained with the approximate

analysis were compared with results from a geometrically-nonlinear finite element analysis.

Specimens with different delamination lengths, delamination depths, and applied loads were considered. In most cases, lateral deflection and G_I obtained with the approximate analysis agreed very well with the finite element results. For the cases in which the agreement was only fair, excellent agreement was obtained by incorporating corrections for rotation of the ends of the delamination.

Before calculating G_I with the approximate analysis, two constants had to be determined from a finite element analysis. Hence, the approximate analysis cannot stand alone (except for calculating lateral deflections). However, a significant advantage of the approximate analysis is that the effect of various parameters on G_I can easily be determined from the governing equations.

REFERENCES

1. Whitcomb, J. D.: Finite Element Analysis of Instability-Related Delamination Growth. NASA TM-81964, 1981.

2. Timoshenko, S. P.; and Gere, J. M.: Theory of Elastic Stability. Second ed., McGraw-Hill Book Co., Inc., New York, 1961, pp. 132-133.

3. Panlilio, F.: Elementary Theory of Structural Strength. John Wiley & Sons, Inc., New York, 1963, p. 273.

4. Lawn, B. R.; and Wilshaw, T. R.: Fracture of Brittle Solids. Cambridge University Press, Cambridge, 1975, p. 62.

5. Rybicki, E. F.; and Kanninen, M. F.: A Finite Element Calculation of Stress Intensity Factors by a Modified Crack Closure Integral. Engineering Fracture Mechanics, vol. 9, no. 4, 1977, pp. 931-938.

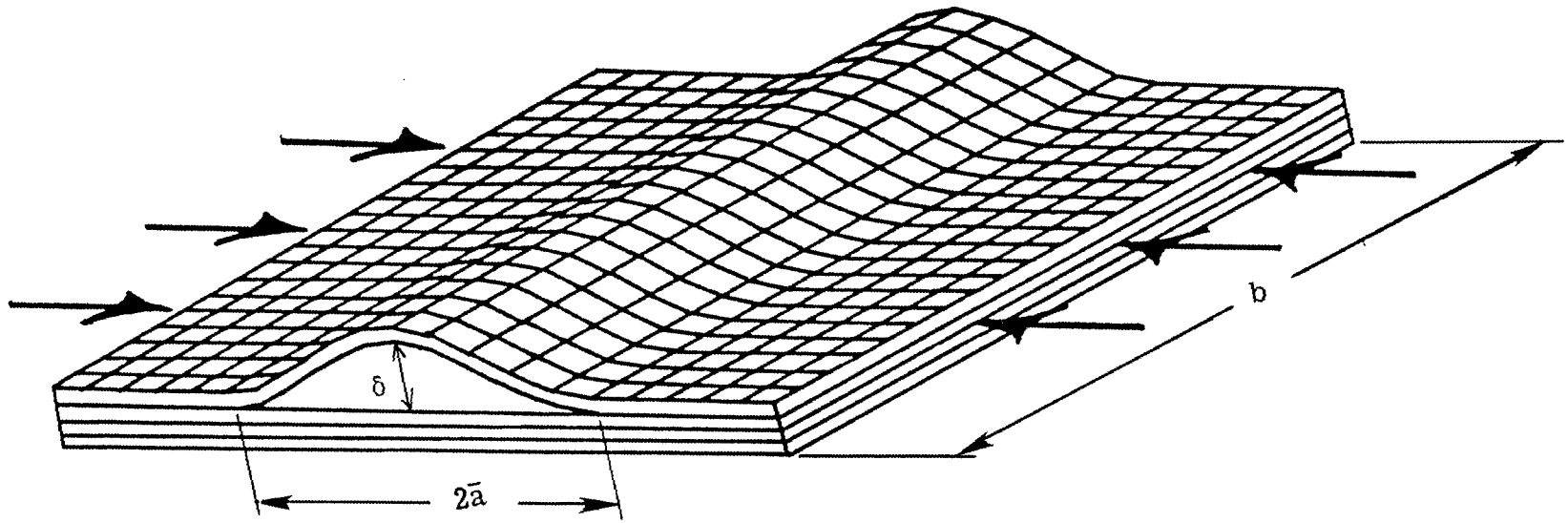

Figure 1.- Local buckling of laminate with through-width delamination.

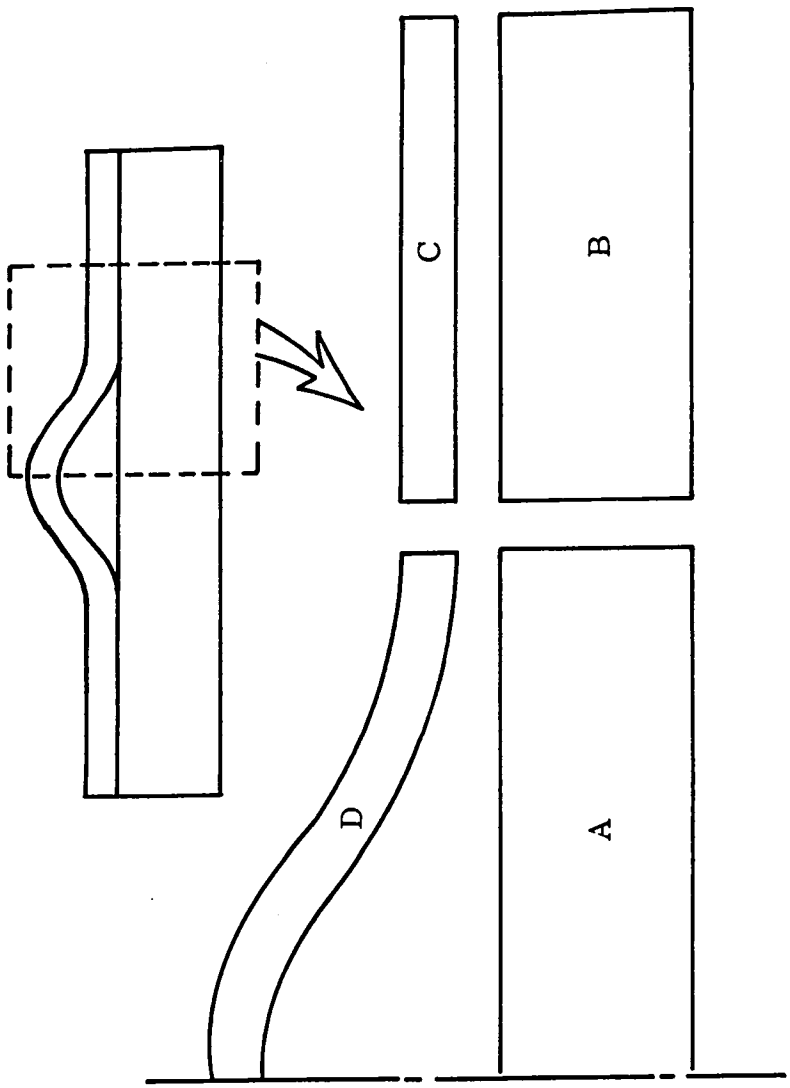

Figure 2.- Subdivision of laminate.

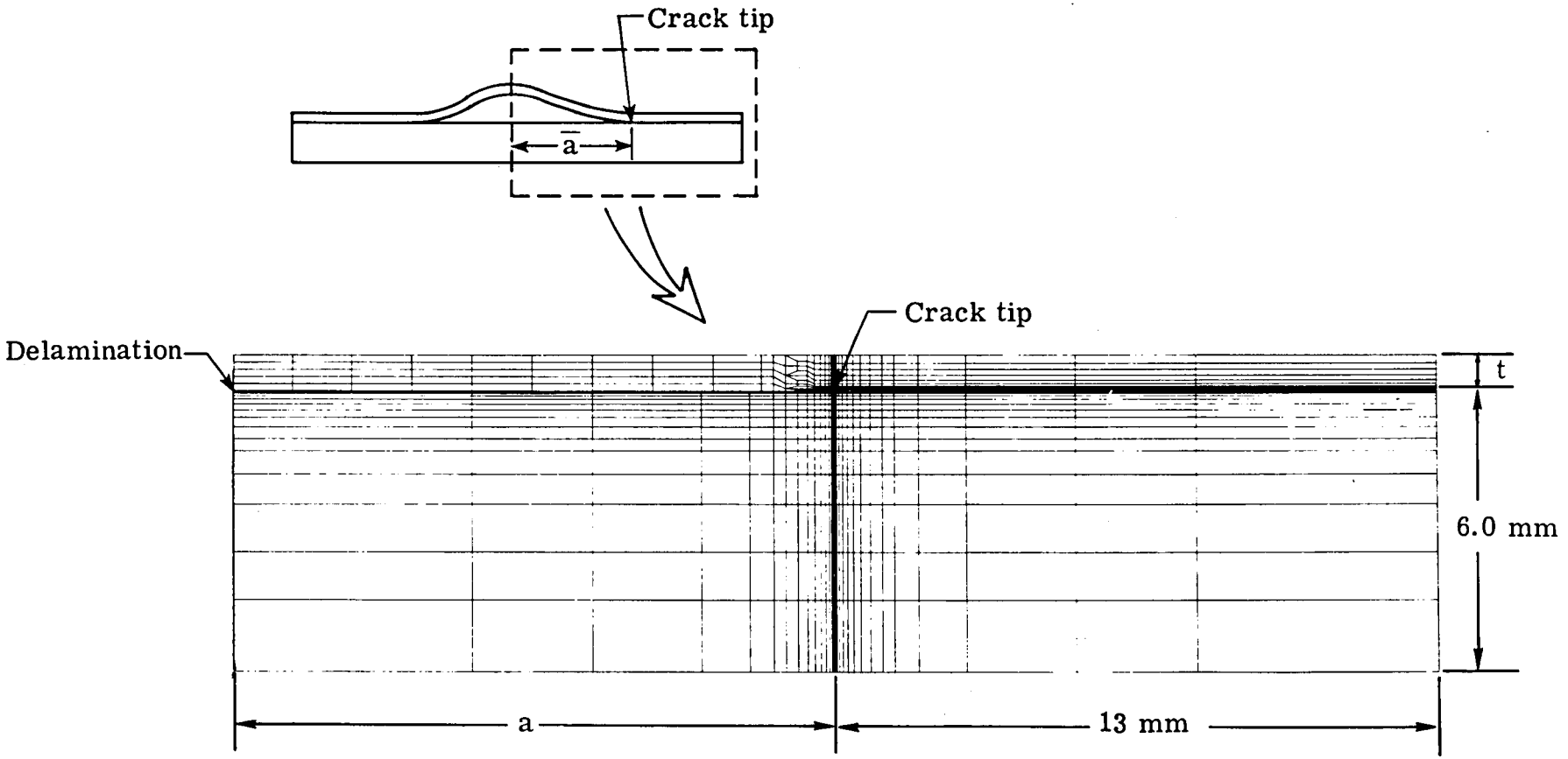

Figure 3.- Typical finite element mesh (In this case 2a = 25.4 mm, t = .762 mm.)

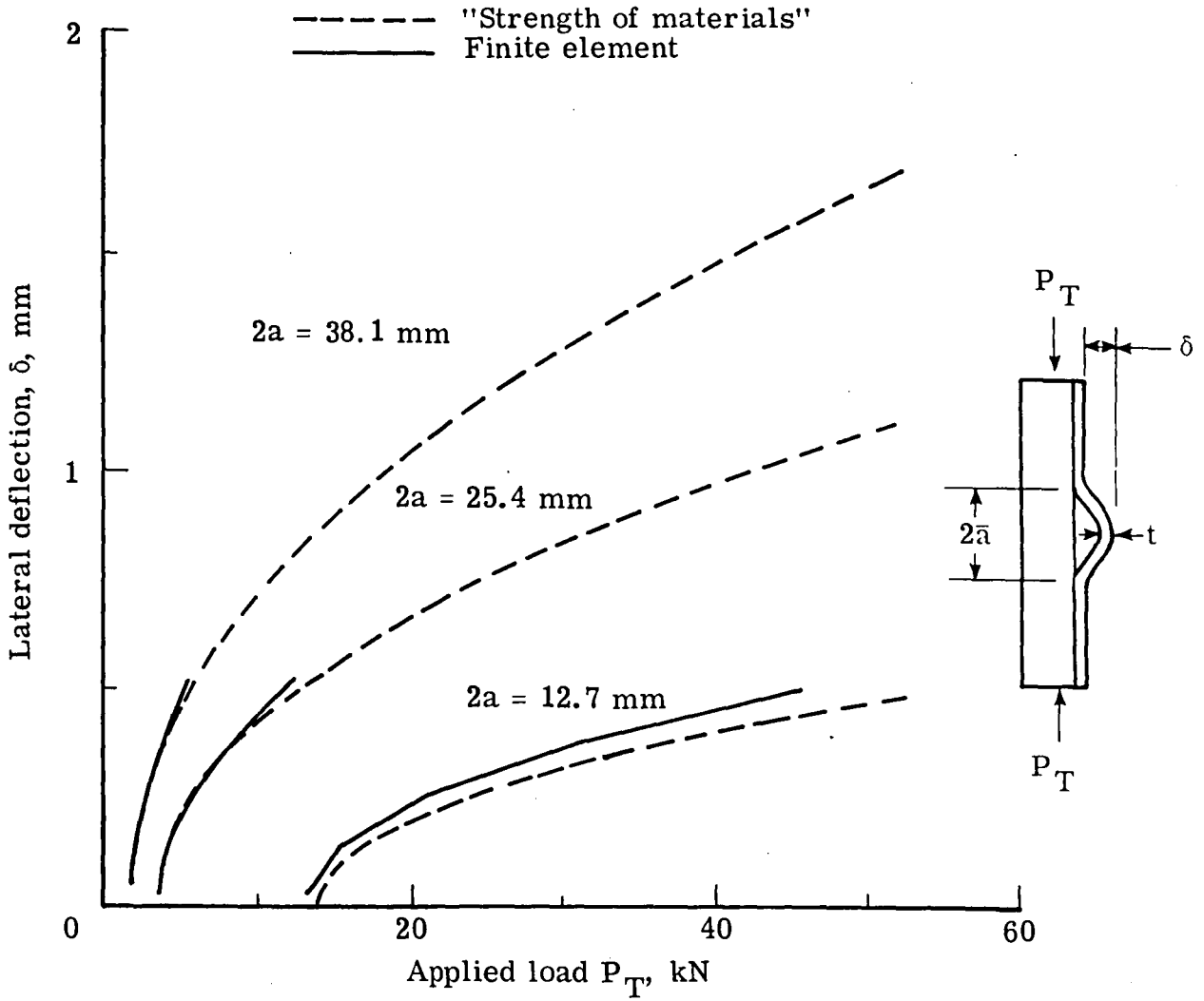

Figure 4.- Lateral deflection versus applied load for several delamination lengths (t = .254 mm).

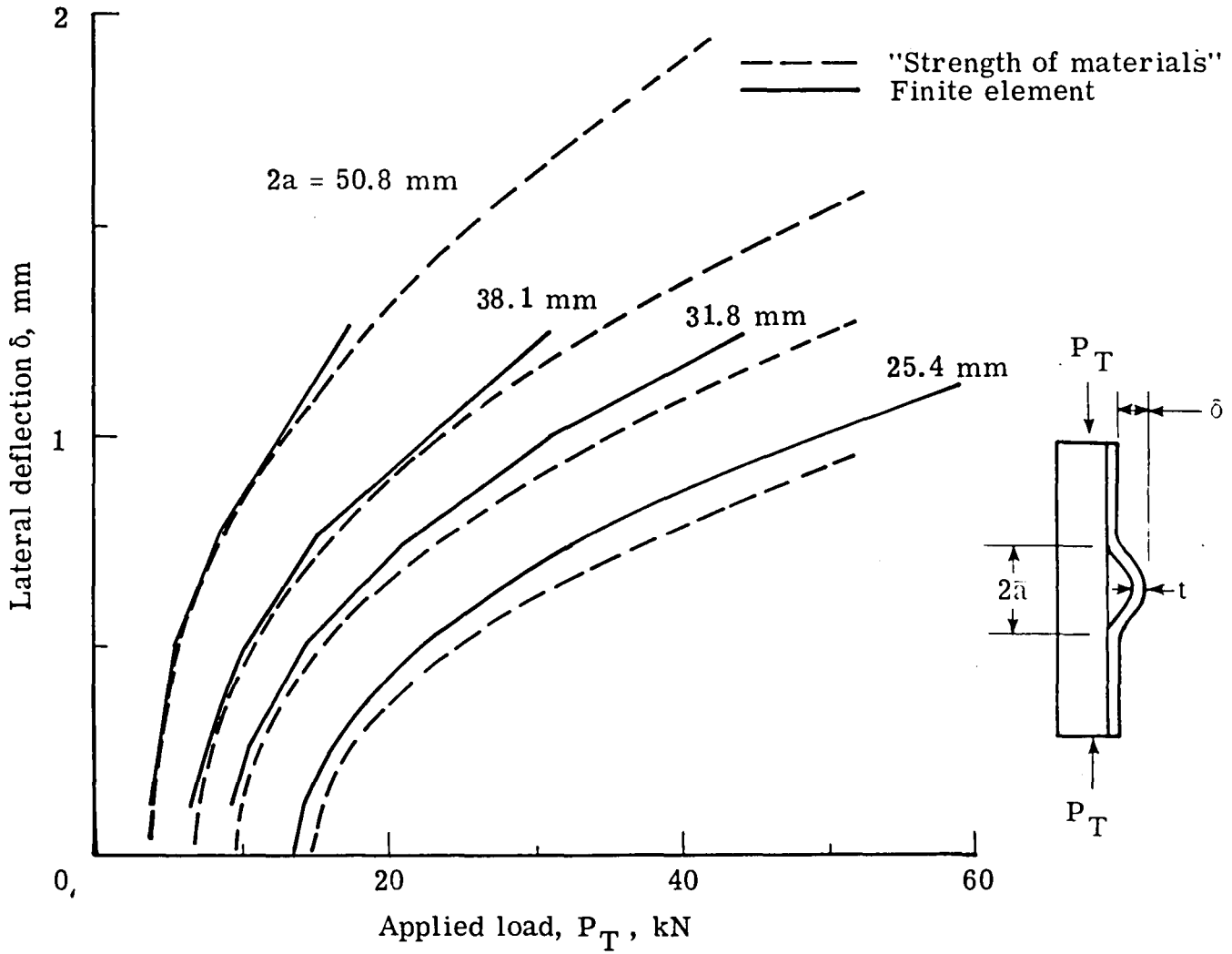

Figure 5.- Lateral deflection versus applied load for several delamination lengths (t = .508 mm) .

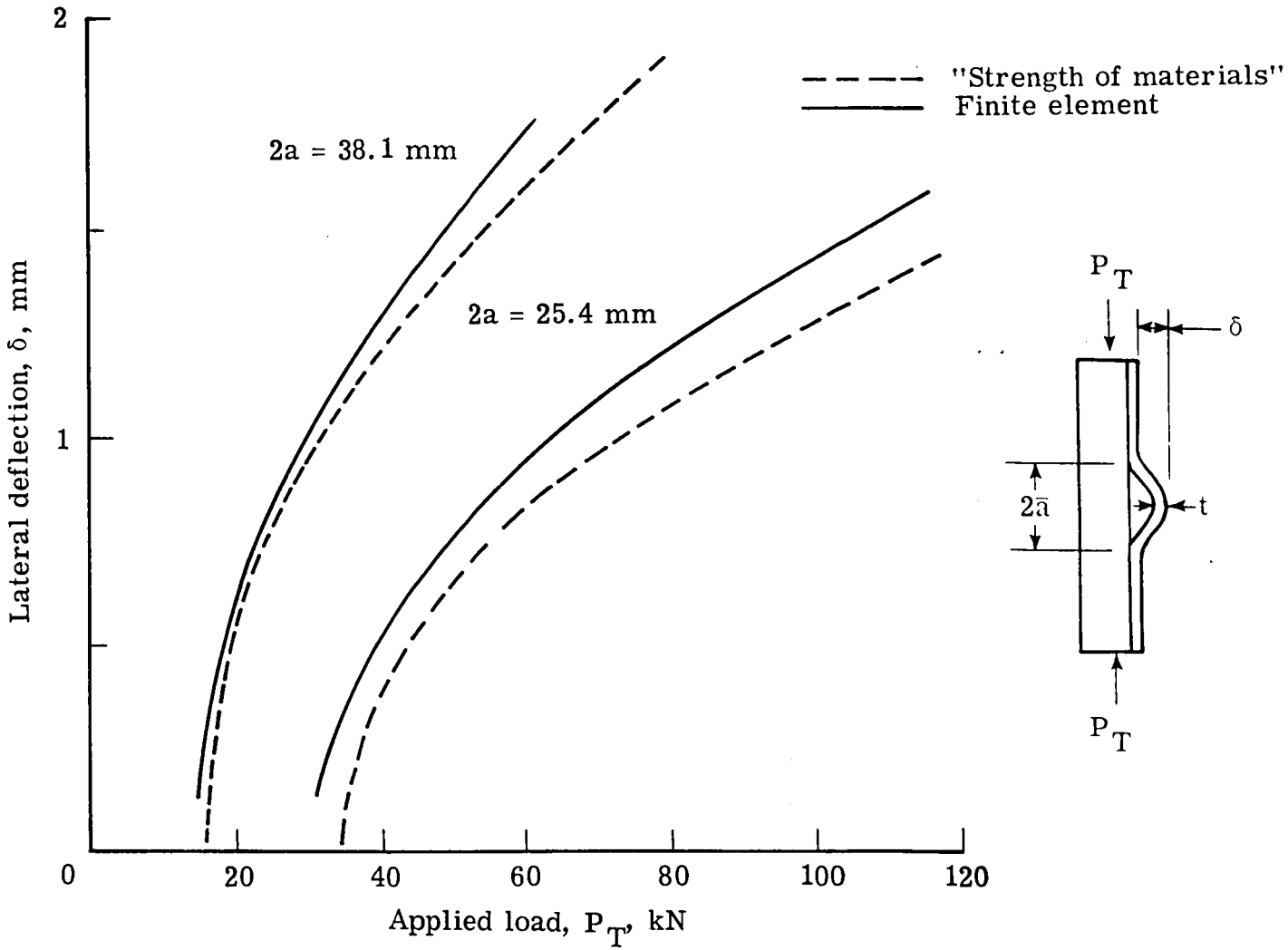

Figure 6.- Lateral deflection versus applied load for two delamination lengths (t = .762 mm).

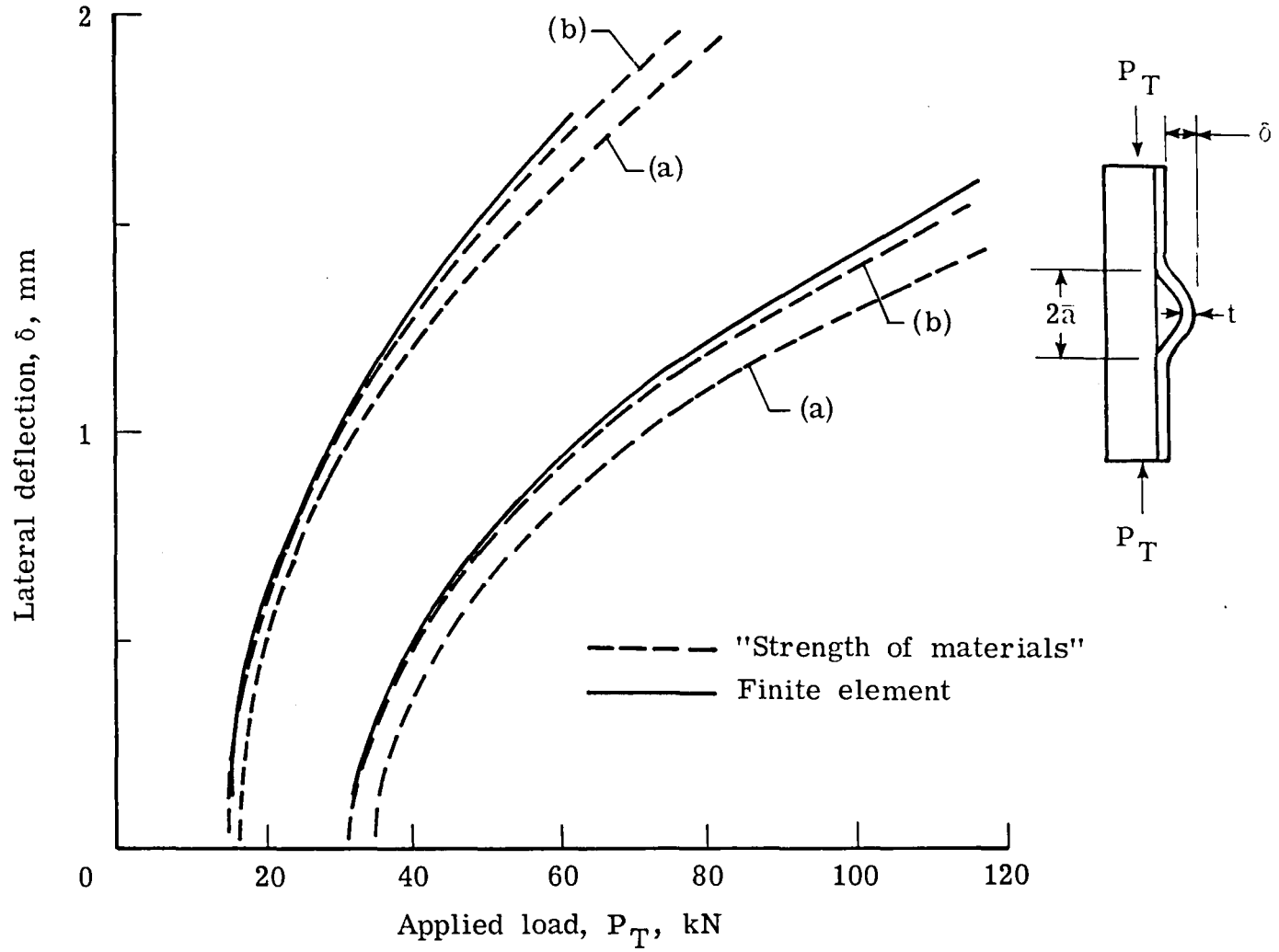

Figure 7.- Lateral deflection vs. load for two delamination lengths. Two versions of the "Strength of materials" solution are shown: (a) without correction for end rotations (b) with correction for end rotations (t = .762 mm).

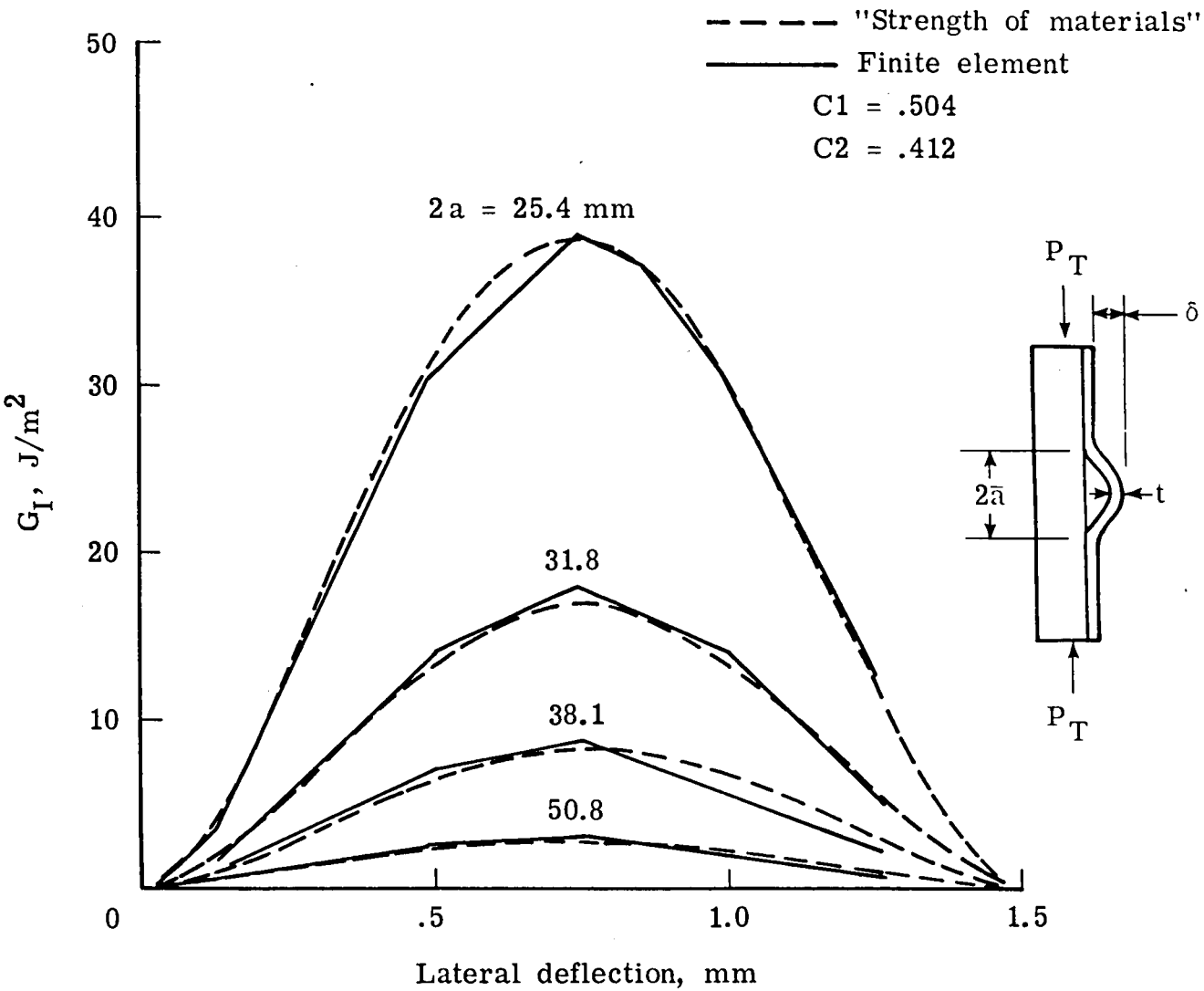

Figure 8.- Relationship between G_I, lateral deflection, and delamination length. (t = .508 mm).

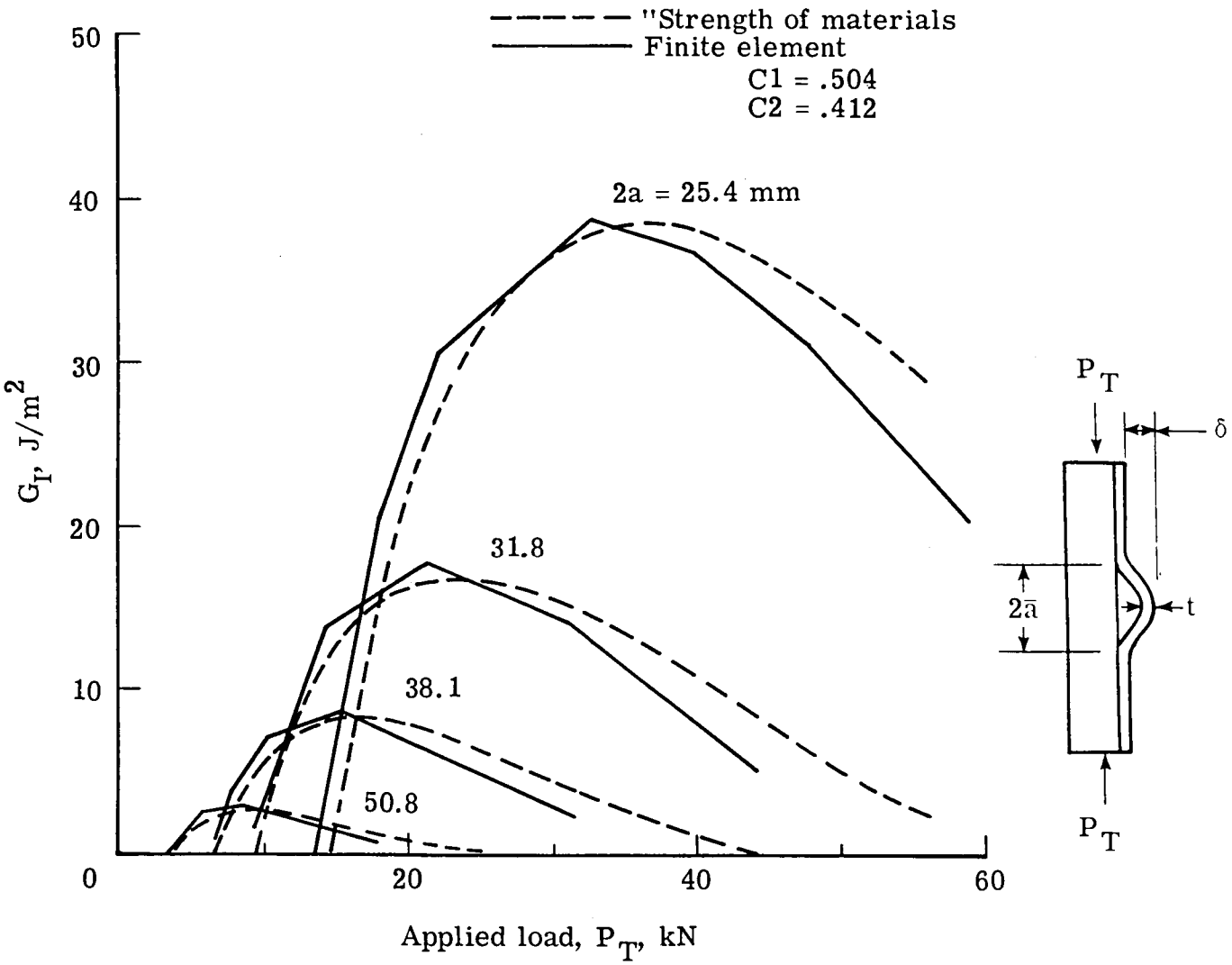

Figure 9.- Relationship between G_I, applied load, and delamination length (t = .508 mm).

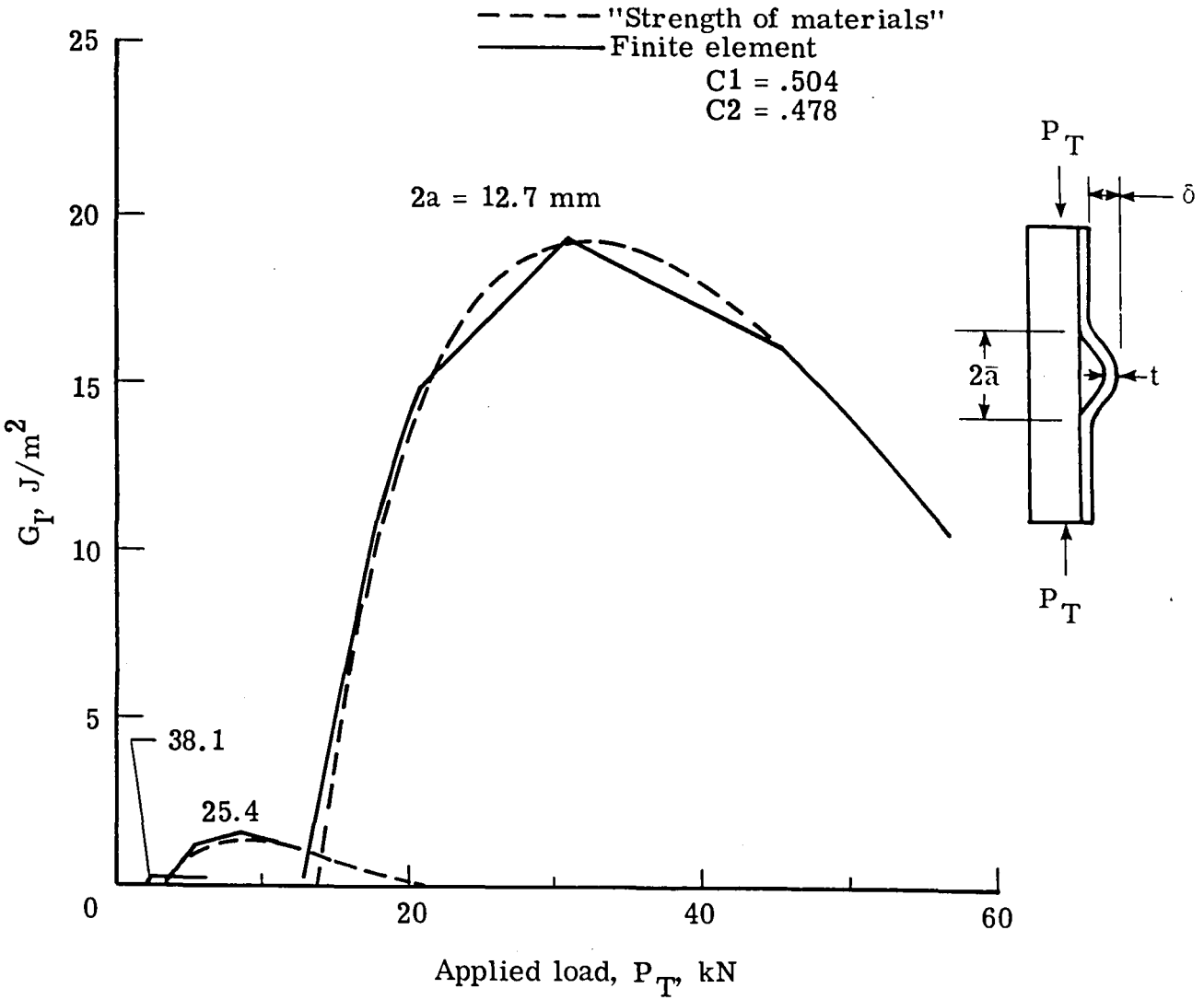

Figure 10.- Relationship between G_I, applied load, and delamination length (t = .254 mm).

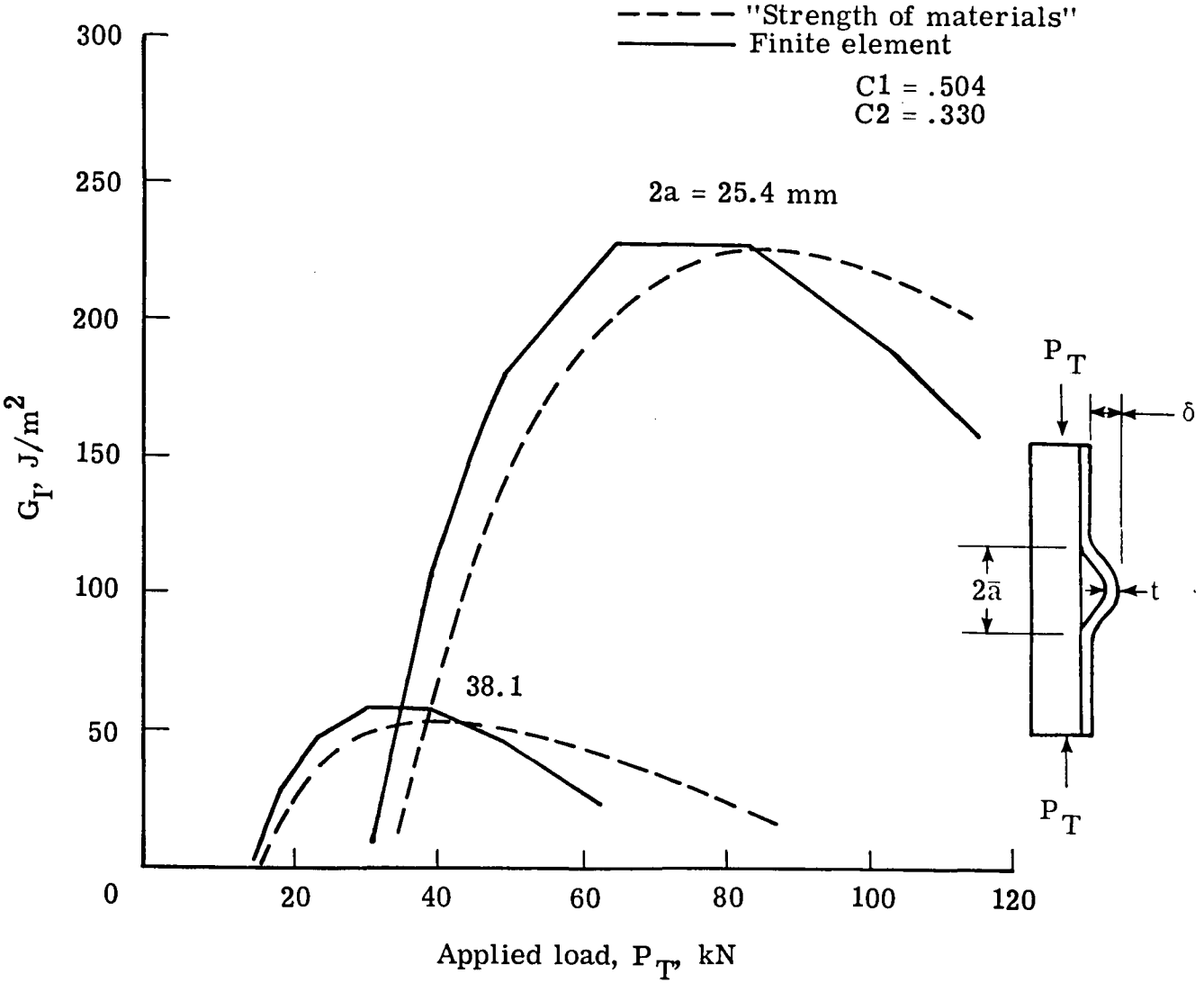

Figure 11. - Relationship between G_I, applied load, and delamination length (t = .762 mm).

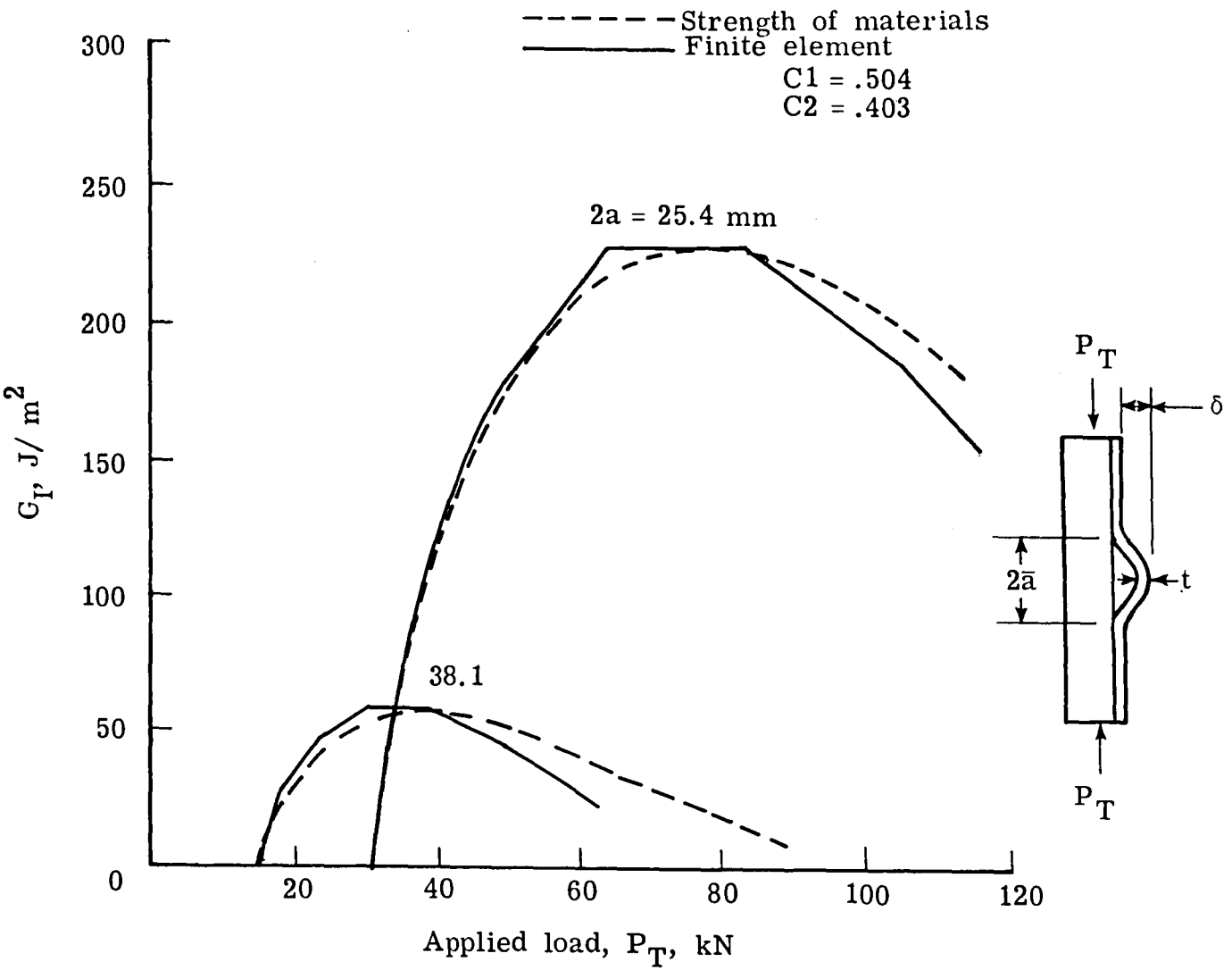

Figure 12.- G_I versus load for two delamination lengths. Strength of materials solution has correction for end rotation (t = .762 mm).

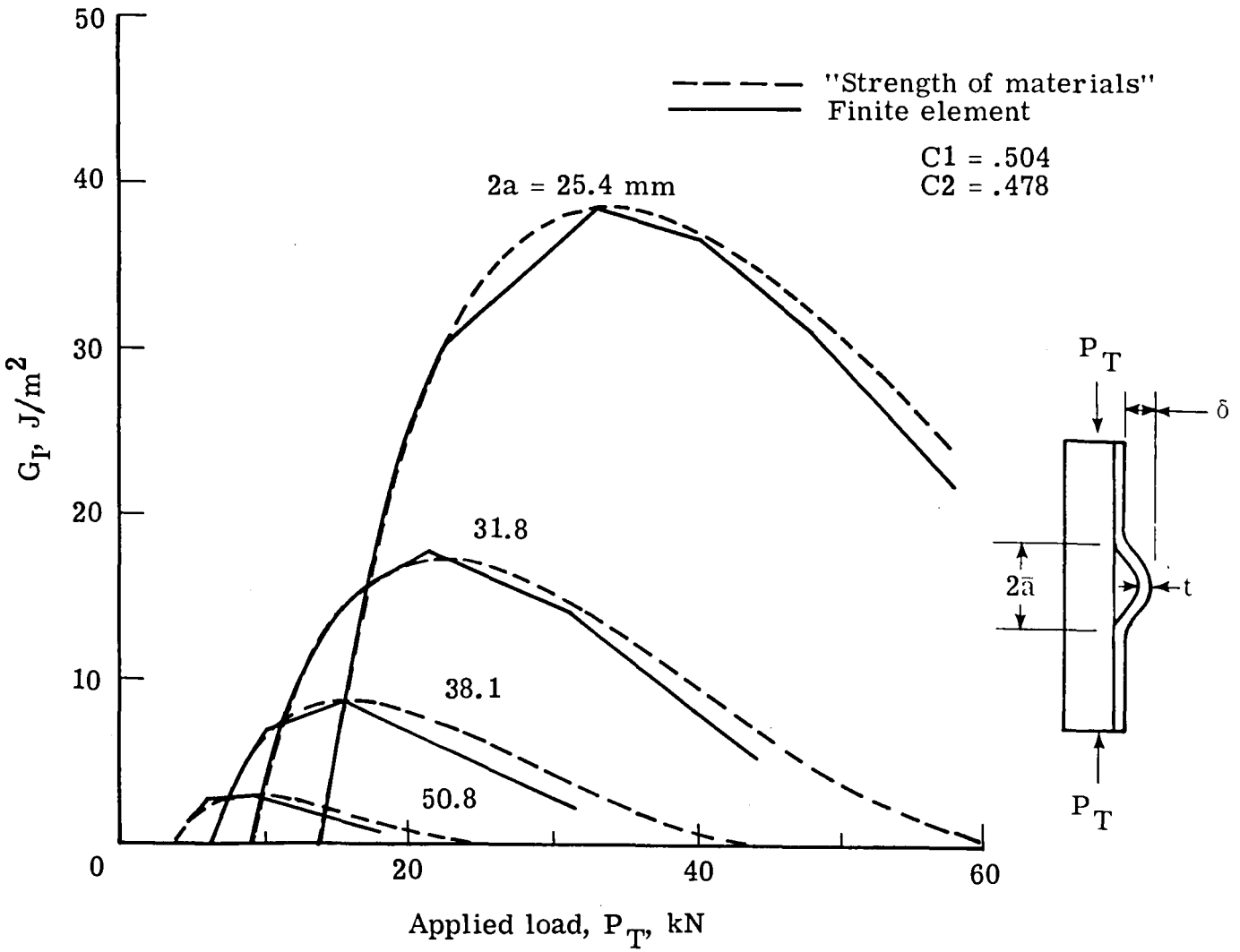

Figure 13.- G_I versus applied load for several delamination lengths. The "Strength of materials" solution has corrections for end rotation (t = .508 mm).

1. Report No.	2. Government Accession No.	3. Recipient's Catalog No.
NASA TM-83147		

4. Title and Subtitle	5. Report Date
APPROXIMATE ANALYSIS OF POSTBUCKLED THROUGH-WIDTH DELAMINATIONS	June 1981
	6. Performing Organization Code 506-53-23-05
7. Author(s)	8. Performing Organization Report No.
John D. Whitcomb	
	10. Work Unit No.
9. Performing Organization Name and Address	
NASA Langley Research Center Hampton, VA 23665	11. Contract or Grant No.
	13. Type of Report and Period Covered
12. Sponsoring Agency Name and Address	Technical Memorandum
National Aeronautics and Space Administration Washington, DC 20546	14. Sponsoring Agency Code

15. Supplementary Notes

16. Abstract

An approximate analysis was developed to analyze the postbuckling behavior of through-width delaminations in a laminated coupon. The analysis contains two parameters which are determined using a finite element analysis. After calculating the parameters for a few configurations, the approximate analysis was used to analyze many other configurations. Lateral deflections and mode I strain-energy release rates obtained with the approximate analysis were compared with results from the finite element analysis. For the configurations analyzed, the approximate analysis agreed very well with the finite element results.

17. Key Words (Suggested by Author(s))	18. Distribution Statement
Composite materials Local buckling Nonlinear stress analysis Laminates Delamination	Unclassified - Unlimited Subject Category 24

19. Security Classif. (of this report)	20. Security Classif. (of this page)	21. No. of Pages	22. Price*
Unclassified	Unclassified	30	A03

* For sale by the National Technical Information Service, Springfield, Virginia 22161

End of Document